

Accepted Manuscript

Precursor solution volume-dependent ligand-assisted synthesis of $\text{CH}_3\text{NH}_3\text{PbBr}_3$ perovskite nanocrystals

Yun Tang, Nan Yan, Zhiwei Wang, Hudie Yuan, Yalou Xin, Hongfeng Yin



PII: S0925-8388(18)33292-4

DOI: [10.1016/j.jallcom.2018.09.054](https://doi.org/10.1016/j.jallcom.2018.09.054)

Reference: JALCOM 47473

To appear in: *Journal of Alloys and Compounds*

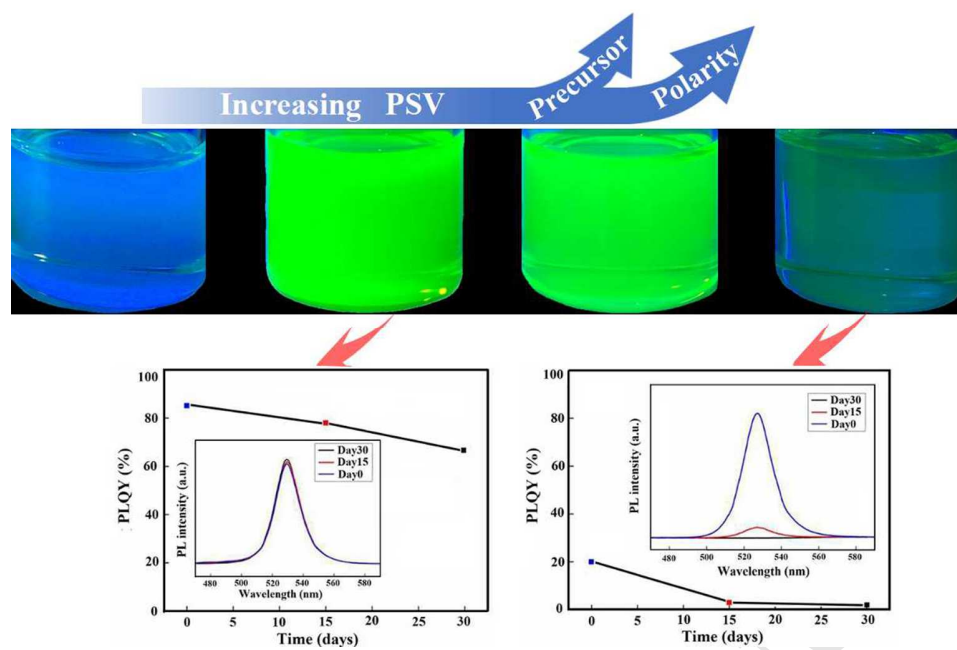
Received Date: 30 April 2018

Revised Date: 31 August 2018

Accepted Date: 5 September 2018

Please cite this article as: Y. Tang, N. Yan, Z. Wang, H. Yuan, Y. Xin, H. Yin, Precursor solution volume-dependent ligand-assisted synthesis of $\text{CH}_3\text{NH}_3\text{PbBr}_3$ perovskite nanocrystals, *Journal of Alloys and Compounds* (2018), doi: 10.1016/j.jallcom.2018.09.054.

This is a PDF file of an unedited manuscript that has been accepted for publication. As a service to our customers we are providing this early version of the manuscript. The manuscript will undergo copyediting, typesetting, and review of the resulting proof before it is published in its final form. Please note that during the production process errors may be discovered which could affect the content, and all legal disclaimers that apply to the journal pertain.



Precursor solution volume-dependent ligand-assisted synthesis of $\text{CH}_3\text{NH}_3\text{PbBr}_3$ perovskite nanocrystals

Yun Tang, Nan Yan, Zhiwei Wang, Hudie Yuan, Yalou Xin, Hongfeng Yin*

College of Materials & Mineral Resources, Xi'an University of Architecture & Technology, Xi'an, Shaanxi, 710055, China

**Corresponding author. E-mail: yinhongfeng@xauat.edu.cn.*

ABSTRACT

Ligand-assisted reprecipitation (LARP) technique is a powerful approach for the synthesis of organometal halide perovskite nanocrystals (PNCs). The morphology and surface property of the formed PNCs which determine their optical properties are ultrasensitive to the synthetic parameters. To guarantee the batch-to-batch reproducibility of PNCs with excellent optical properties, it is of central importance to better understand the factors influencing the formation of PNCs during LARP process. Herein the dual-factor of the amount of perovskite precursor and the polarity of mixture solvent was modified by varying precursor solution volume (PSV) in the LARP system. The concentration, size, surface state and optical properties of the synthesized $\text{CH}_3\text{NH}_3\text{PbBr}_3$ PNCs as a function of PSV were systematically investigated aiming to understand the influence of the dual-factor on the nucleation and growth of PNCs. Experimental results revealed that few crystal nuclei was generated due to lower amount of precursor at lower PSV, which was favorable for the growth of large perovskite crystals. At the higher PSV, the inhibition of crystal growth with increased amount of precursor was compensated by increasing the polarity of mixture solvent, which led to the dissolution of surface ligands and eventually growth

of large perovskite crystals. The obtained results on PSV-dependent synthesis of PNCs will be used as a guide to optimize the synthetic parameters in the LARP process.

Keywords: Perovskite nanocrystals; Ligand-assisted reprecipitation; Dual-factor; Nucleation; Growth; Optical property

1. Introduction

Organometal trihalide perovskites $\text{CH}_3\text{NH}_3\text{PbX}_3$ ($\text{X}=\text{Cl}, \text{Br}, \text{I}$) materials are attractive semiconductor materials with excellent optical and electrical properties and great potential for a diverse range of applications in photovoltaics [1-6], light-emitting diodes [7-9], laser [10,11], and photodetectors [12-14]. When reducing the dimension of $\text{CH}_3\text{NH}_3\text{PbX}_3$ from bulk to nanoscale, i.e., in the quantum confined space, the $\text{CH}_3\text{NH}_3\text{PbX}_3$ perovskite nanocrystals (PNCs) begin to display extraordinary optical properties, including tunable emission over the entire visible spectrum, narrow emission linewidth and high quantum efficiency [15]. Over the past few years, a vast body of research has been carried out mainly on synthesis and optical properties of PNCs. Since Galian and Perez-Prieto first reported the fabrication of $\text{CH}_3\text{NH}_3\text{PbBr}_3$ PNCs using organic ammonium cations as capping ligands by hot-injection method in 2014 [16], solution-based approaches have been extensively investigated to synthesize PNCs with various shapes, sizes and dimensions [17-23].

Ligand-assisted reprecipitation (LARP) technique is one of the most convenient solution approaches, in which the formation of PNCs can be accomplished within a few seconds without the needs of heating or protective atmosphere [9]. LARP is

usually conducted by mixing the precursor solution consisting of a polar solvent, perovskite precursor and organic ligand, with a nonpolar solvent under vigorous stirring at room temperature. Due to the different solubility of CH_3NH_3^+ , Pb^{2+} , X^- in polar and nonpolar solvent, the mixing produces a highly supersaturated state immediately and then induces fast nucleation and growth of $\text{CH}_3\text{NH}_3\text{PbX}_3$ PNCs. Various synthetic parameters play a crucial role in the morphology and surface property of resulting PNCs. For example, size-tunable $\text{CH}_3\text{NH}_3\text{PbBr}_3$ PNCs were synthesized through varying the temperature of the nonpolar solvent [18], the precursor and ligand concentrations [19], or the ratio of $\text{CH}_3\text{NH}_3\text{Br}$ to PbBr_2 in the perovskite precursor [20]. In addition, a variety of ligands, polar and nonpolar solvents were employed to fabricate $\text{CH}_3\text{NH}_3\text{PbI}_3$ and $\text{CH}_3\text{NH}_3\text{PbBr}_3$ PNCs with different shape and surface state [21]. Thus, in order to guarantee the batch-to-batch reproducibility of PNCs achieve excellent properties, it is of central importance to better understand the related synthetic parameters influencing the LARP process.

Although the influence of single factor on LARP process has been well-established, understanding of the combined effect of several factors is also important because practical synthesis of PNCs usually involves the variation of more than one factor. The precursor and the polarity of the reaction system are two important parameters during LARP process, while the combined effects of both factors on the synthesis and optical properties of $\text{CH}_3\text{NH}_3\text{PbX}_3$ PNCs are still poorly understood. Herein, different precursor solution volume (PSV) was introduced to modify the amount of precursor and the polarity of the mixture solvent at the same

time. The concentration, size, surface state and optical properties of $\text{CH}_3\text{NH}_3\text{PbBr}_3$ PNCs synthesized with different PSV were systematically investigated, aiming to understand the influence of the dual-factor on the nucleation and growth of PNCs. The experimental results will be used as a guide to optimize the related synthetic parameters in the LARP process.

2. Experimental

2.1. Materials

Lead(II) bromide (PbBr_2 , 99%), methylamine (CH_3NH_2 , 33 wt% in absolute ethanol), hydrobromic acid (HBr, 48 wt% in water), N,N-Dimethylformamide (DMF, analytical grade, 99.5%), oleic acid (OA, analytical grade) and n-octylamine (99%) were purchased from Aladdin Reagent Company. Analytical grade toluene and diethylether were purchased from Beijing Chemical Reagent Company. All the chemicals were used without further purification.

2.2. Synthesis of $\text{CH}_3\text{NH}_3\text{Br}$ and $\text{CH}_3(\text{CH}_2)_7\text{NH}_3\text{Br}$ (OABr)

The $\text{CH}_3\text{NH}_3\text{Br}$ or $\text{CH}_3(\text{CH}_2)_7\text{NH}_3\text{Br}$ was synthesized through the reaction of CH_3NH_2 or n-octylamine with HBr based on previous work [24, 25]. The synthesis of $\text{CH}_3\text{NH}_3\text{Br}$ is listed as follows: The reaction solution consisting of CH_3NH_2 and HBr with the molar ratio of 1:1 was stirred for 2 h in an ice bath followed by vacuum drying. The obtained slight yellow precipitates were washed three times with diethylether and dried under vacuum condition to get purified white powders. OABr

was prepared using the same method by mixing n-octylamine and HBr in a 1:1 molar ratio.

2.3. Synthesis of $\text{CH}_3\text{NH}_3\text{PbBr}_3$ PNCs

$\text{CH}_3\text{NH}_3\text{PbBr}_3$ PNCs were fabricated following the reported LARP technique [9]. 0.16 mmol $\text{CH}_3\text{NH}_3\text{Br}$ and 0.2 mmol PbBr_2 were dissolved in 5 mL DMF (polar solvent) with 0.5 mL OA and 0.08 mmol OABr to form a clear precursor solution. Then, variable volume (0.5, 1, 2 mL) of precursor solution was dropped into 10 mL toluene as a nonpolar solvent under vigorous stirring at room temperature. After centrifugation at 7000 rpm for 5 min to discard the precipitates, green or yellow-green $\text{CH}_3\text{NH}_3\text{PbBr}_3$ PNCs solutions were obtained.

2.4. Characterizations

The X-ray diffraction (XRD) patterns were taken on a X-ray powder diffractometer (D/Max 2200V, Japan) using a CuK_α ($\lambda=1.5405981\text{\AA}$) radiation source. The XRD samples were prepared by drop casting PNCs solutions onto quartz sample holder and dried overnight. Liquid samples deposited on amorphous carbon-coated copper grids were analyzed using a FEI Tecnai G2 F20 transmission electron microscopy (TEM) instrument operating at an acceleration voltage of 200 kV. The morphology of the precipitate was observed using scanning electron microscopy (SEM, SU8010, Hitachi, Japan). The X-ray photoelectron spectroscopy (XPS) data was collected on a X-ray photoelectron spectrometer (K-Alpha, Thermo Electron Corporation, USA). The C 1s peak at 284.8 eV was set as a reference for all XPS peak positions. The SEM and XPS samples were prepared by drop casting PNCs solutions

on silicon wafers and also dried overnight. The UV-vis absorption spectra were obtained on a spectrophotometer (U-3310UV, Hitachi, Japan) and photoluminescence (PL) spectra were measured on a fluorescence spectrophotometer (F-4500, Hitachi, Japan). The absolute PL quantum yield (PLQY) was determined by quantum yield measurement system (C9920-02G, Hamamatsu, Japan) with an integrating sphere at room temperature.

3. Results and discussion

3.1. LARP synthesis of $\text{CH}_3\text{NH}_3\text{PbBr}_3$ PNCs

Different volumes of precursor solution containing a fixed concentration of $\text{CH}_3\text{NH}_3\text{PbBr}_3$ precursor (PbBr_2 and $\text{CH}_3\text{NH}_3\text{Br}$) and organic ligands (OA and OABr) were dropped into a vigorously stirred toluene solvent at room temperature. Once the precursor solution was mixed with the toluene, the color of the mixture became bright green immediately in all cases, which indicated the formation of perovskite crystals. After removing the relatively larger particles by centrifugation, clear supernatant solutions with different concentration of PNCs were obtained. It should be noted that the amount of the precipitate was found to increase accompanying with higher PSV in the reaction mixture (28, 42 and 60 mg per batch using 0.5, 1 and 2 mL precursor solution, respectively). Fig. 1a and 1b present the $\text{CH}_3\text{NH}_3\text{PbBr}_3$ PNCs solutions synthesized with different PSV under normal indoor light and UV light illumination. The solutions show bright luminescence under UV light using PSV of 0.5 or 1 mL. In contrast, the luminescence intensity of PNCs solution obtained from 2 mL precursor

solution is substantially lower, indicating a lower concentration of PNCs, which is also consistent with the higher amount of the precipitate. The crystal structure of the synthesized $\text{CH}_3\text{NH}_3\text{PbBr}_3$ PNCs and the corresponding discarded precipitate was characterized by XRD, as shown in Fig. 1c. Both the as-prepared $\text{CH}_3\text{NH}_3\text{PbBr}_3$ PNCs and the precipitate possess a cubic structure (space group, Pm-3m). The XRD peaks located at 2θ of 14.9° , 21.2° and 30.6° can be assigned to the diffractions from (100), (110) and (200) planes, respectively. The sharp diffraction peaks from the precipitate indicate the formation of perovskite crystals with large particle size based on Debye-Scherrer equation, as also observed in Fig. 1d. In contrast, the full width at half maximum (FWHM) of the diffraction peaks become broader for PNCs, and the crystallinity decreases, corresponding to the small particle size and the superimposition of background peak originating from organic ligands [26].

Fig. 1e shows the UV-vis absorption and PL spectra of $\text{CH}_3\text{NH}_3\text{PbBr}_3$ PNCs synthesized with different PSV. The absorption onsets are all around 520 nm. The optical band gaps, measured from the absorption data using Tauc plot $((\alpha h\nu)^2 \text{ vs } h\nu$ for a direct allowed transition, where α is absorption coefficient, h is Planck's constant, and ν is frequency of incident photons) are 2.3-2.35 eV. The PL emission spectra show peak positions at 526-528 nm (FWHM=20 nm) with excitation at 350 nm. Thus, the PNCs have a small Stokes shift (5-8 nm) between the absorption and the emission peak, which is consistent with a direct exciton recombination process. Additionally, the gradually reduced absorbance is observed with the increasing PSV, which could be also associated with the decreased concentration of PNCs in solution.

In order to further find out the relationship between PSV and PNCs concentration, 0.1 mL precursor solution was also introduced in LARP system. After mixing and centrifugation, a high amount of precipitate and a colorless supernatant were obtained, indicating substantially low concentration of PNCs in solution. It is known that the formation of perovskite particle is realized by supersaturation and following rapid nucleation and growth processes. According to LaMer and Dinegar's model, the nucleation and growth of PNCs is highly dependent on the precursor concentration, reaction temperature, etc [27]. Herein, the dual-factor of amount of precursor and polarity of the mixture solvent becomes the key factor governing the two processes. At the PSV of 0.1 mL, few crystal nuclei are generated in the mixture due to the low amount of precursor, which is favorable for the growth of perovskite crystals, and hence leads to low concentration of PNCs. With the increase of PSV, both the amount of precursor and the polarity of the mixture solvent which relevant to the ratio of DMF to toluene are increased. When increased the volume to 2 mL, on one hand, a large amount of nuclei would generate in a short period as a result of supersaturation, which could suppress the growth of perovskite particles. On the other hand, the mixture solvent with high polarity could help to activate the particle surface by dissolving the surface ligands, which in turn promote the growth of perovskite particles. The obtained low concentration of PNCs in solution demonstrates the dominant effect of high polarity on the growth of PNCs. In contrast, at the PSV of 0.5 mL, a large amount of nuclei are produced, most of the grains grow up to the nanometer level. Besides, the low polarity of mixture solvent may have less effect on

the surface ligands of the particles. Compared to 0.1 and 2 mL of PSV, the 0.5 mL sample has the highest yield of PNCs concentration. Thus, in order to achieve high concentration of PNCs, it is of importance to manipulate the PSV to the optimized range in the LARP process.

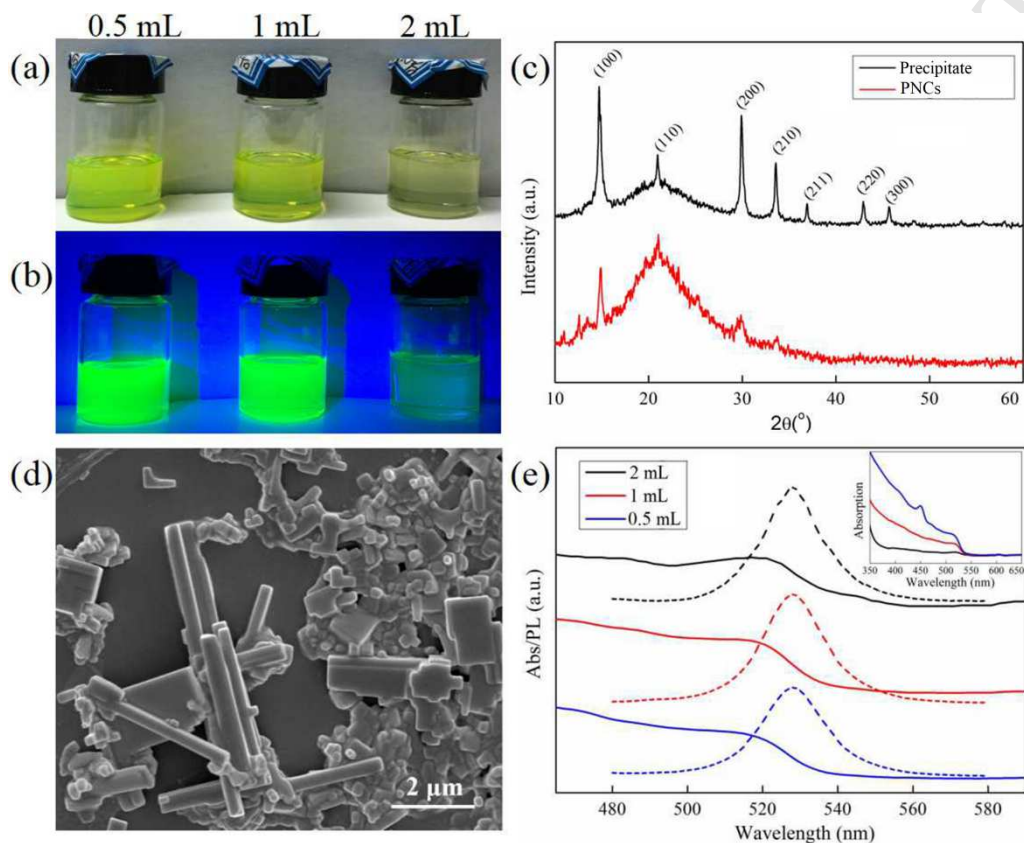


Fig. 1. Photographic images of the $\text{CH}_3\text{NH}_3\text{PbBr}_3$ PNCs solutions synthesized with different PSV under (a) normal indoor light or (b) UV light illumination. (c) XRD patterns of PNCs synthesized with 0.5 mL precursor solution and the corresponding precipitate. (d) SEM image of the precipitate. (e) UV-vis absorption and PL spectra of the $\text{CH}_3\text{NH}_3\text{PbBr}_3$ PNCs solutions and the inset shows the comparison of absorbance of PNCs synthesized with different PSV.

3.2. Characterization of $\text{CH}_3\text{NH}_3\text{PbBr}_3$ PNCs

TEM was employed to exam the structure and morphology of the prepared $\text{CH}_3\text{NH}_3\text{PbBr}_3$ PNCs. The corresponding TEM, high resolution TEM (HR-TEM) images and size distribution (each obtained on 100 particles) are shown in Fig. 2. All PNCs exhibit spherical shape. The HR-TEM images of $\text{CH}_3\text{NH}_3\text{PbBr}_3$ PNCs present

clear lattice fringes, which suggest a highly crystalline structure. The interplanar distances of 2.91 and 2.92 Å in HR-TEM images are very close to that of (002) plane measured by XRD (2.95 Å). The average diameter of $\text{CH}_3\text{NH}_3\text{PbBr}_3$ PNCs is 7.08 ± 1.1 nm and 5.7 ± 0.5 nm for the 0.5 mL and 2 mL sample, respectively. It is worth noting that PNCs obtained from 2 mL precursor solution possess smaller particle size, which exactly results from the growth inhibition effect caused by the large amount of crystal nuclei mentioned above.

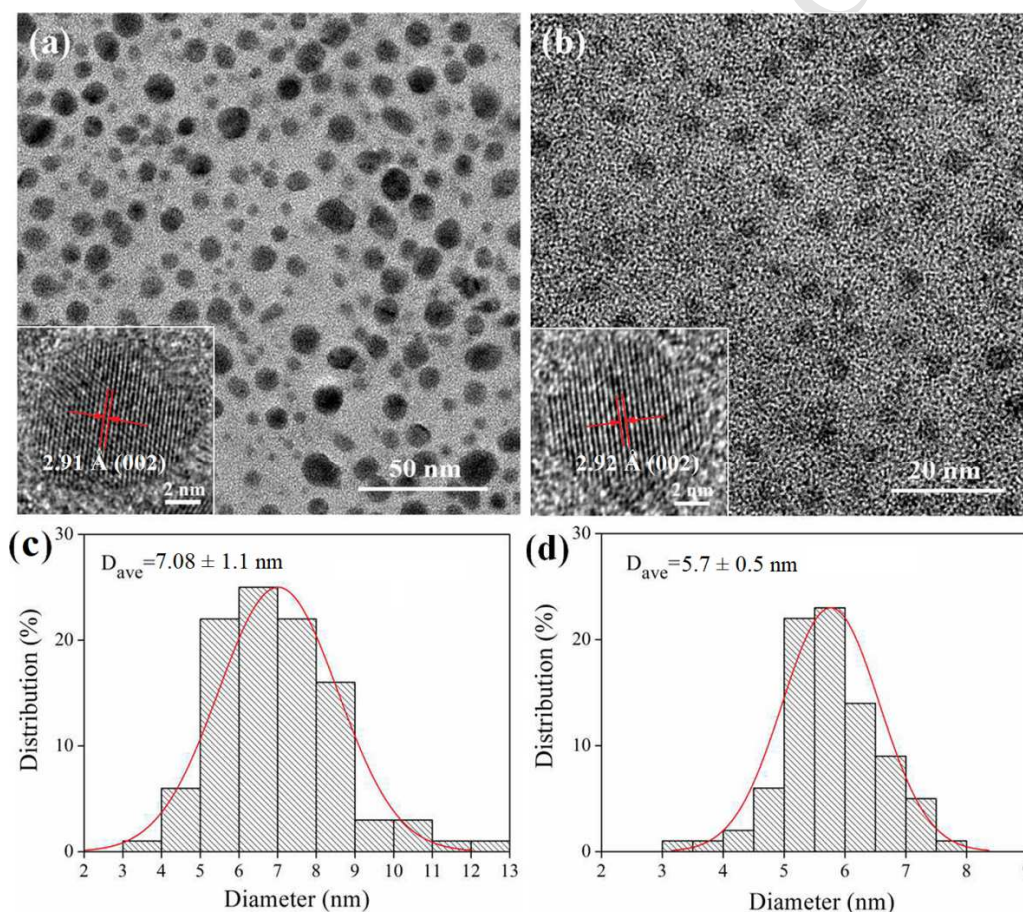


Fig. 2. TEM, HR-TEM images and size distribution histograms of the PNCs synthesized with 0.5 mL (a and c) and 2 mL (b and d) precursor solution.

As for the PNCs synthesized with 2 mL precursor solution, an obvious color change is observed upon dilution with more toluene. As shown in the photographs of Fig. 3a, under UV light illumination, the change is immediately apparent, from light

blue to bright green. The UV-vis absorption spectra in Fig. 3a also indicate an increased absorbance after dilution. According to Beer-Lambert law, the absorbance is proportional to the concentration at linear region. Therefore, we can conclude that the concentration of $\text{CH}_3\text{NH}_3\text{PbBr}_3$ PNCs in the 2 mL sample increases upon dilution. Additionally, the PL spectrum of the 2 mL sample displays only one peak at 527 nm, while an additional peak at shorter wavelength appears after dilution, which is not observed in the dilution of the 0.5 mL or 1 mL sample. As mentioned above, the polarity of the mixture solvent increases with the increase of PSV. The perovskite precursor, and especially the ligands on the surface of PNCs may redissolved in such solvent. A subsequent dilution of the 2 mL sample with toluene again leads to the precipitation of $\text{CH}_3\text{NH}_3\text{PbBr}_3$ PNCs. Furthermore, with the higher concentration of the ligands stabilizing the surfaces, the newly formed PNCs possess a much smaller size of 2-4 nm (see Fig. 3b), comparable or smaller than the exciton Bohr diameter of bulk $\text{CH}_3\text{NH}_3\text{PbBr}_3$ (~4 nm). The smaller PNCs with a higher degree of quantum confinement eventually lead to the pronounced blue-shift of new peak as compared to the original one in the PL spectrum [28].

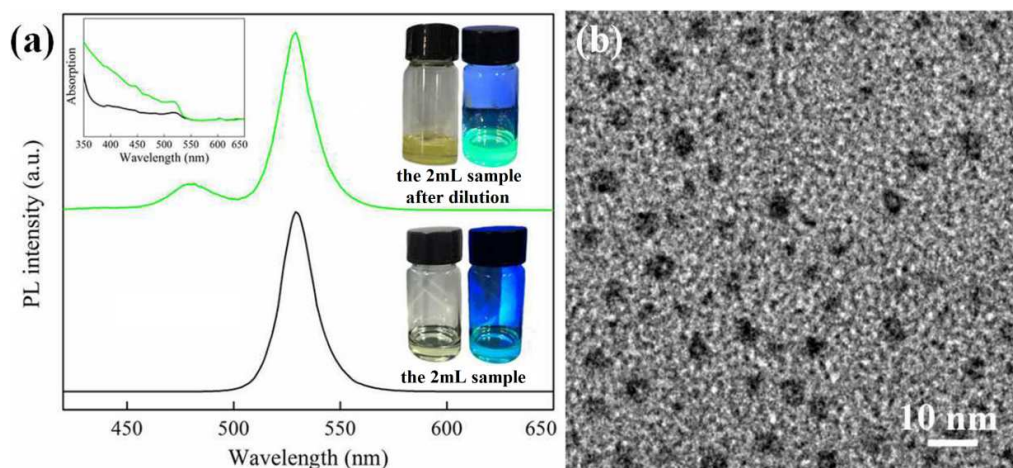


Fig. 3. (a) PL spectra and photographic images under normal indoor light (left) or UV light (right) illumination of the 2 mL sample before and after dilution. The inset shows the comparison of UV-vis absorbance of the 2 mL sample before and after dilution. (b) TEM image of the 2 mL sample after dilution.

XPS analysis was also performed to investigate the surface state of PNCs synthesized with 0.5 or 2 mL precursor solution. As shown in Fig. 4, in both cases, the XPS spectrum of Pb 4f shows two symmetric peaks attributed to Pb 4f_{7/2} and Pb 4f_{5/2} level at binding energies of 138.7 eV and 143.6 eV, respectively. The spin orbit split between the Pb 4f_{7/2} and Pb 4f_{5/2} levels is of 4.87 eV, which is in agreement with the reported value (4.8 eV) in literature [29]. The Br 3d peak can be fitted into two peaks centered at 68.8 and 69.8 eV, corresponding to the inner and surface Br ions, respectively. The O 1s XPS spectrum can also be fitted into two peaks. The lower energy peak at 532.5 eV results from two nonequivalent O atoms in oleic acid (R-COOH), while the higher energy peak at 533.9 eV can be assigned to two chemically equivalent O atoms in carboxylate species of deprotonated oleic acid (R-COO⁻), which could bind to the surface Pb ions based on hard soft acid base (HSAB) theory (see Fig. 4g). Although both R-COO⁻ (borderline base) and Br⁻ (borderline base) can bond with Pb²⁺ (borderline acid), R-COO⁻ can replace the Br⁻ of

PbBr₂ for the binding constant of R-COO⁻ with Pb²⁺ ($\lg k_1=2.52$) is much larger than the second step binding constant for PbBr₂ ($\lg k_2=0.7$) [30]. The N 1s spectrum contains two peaks, implying the two existing chemical states of the N element. The peak at 400 eV can be attributed to the methylamine salt [31], while the peak at 402 eV could be originated from octylamine salt. The octylammonium cation binds to the surface Br presumably through hydrogen bonding or electrostatic interactions (see Fig. 4g) [32-34]. The difference of intensity ratio of these two peaks between the 0.5 mL and 2 mL sample can be attributed to the smaller size and higher specific surface area, thus more amount of the ligands on the surface of the 2 mL sample.

PLQY is an important parameter to evaluate the luminous efficiency of the PNCs. It can be found that the PLQY of as-prepared CH₃NH₃PbBr₃ PNCs exceed 70% in the case of 0.5 mL precursor solution, whereas the PLQY of CH₃NH₃PbBr₃ PNCs synthesized with 2 mL precursor solution reach as low as 20-30%. It is known that the PLQY represents the ratio between radiative and non-radiative recombination in the PNCs, and the enhancement of non-radiative recombination is usually generated by the surface trap states in PNCs. In addition, the presence of OA/OABr ligands serving as surface binding species could passivate the surface defects and prevent nonradiative recombination at surface trap states. In our case, the 0.5 mL sample has more efficient surface ligands coordination for the relatively lower polarity of mixture solvent. Therefore, compared to the 2 mL sample, PNCs synthesized with 0.5 mL precursor solution possess a relatively inert, well passivated particle surface and thus higher PLQY.

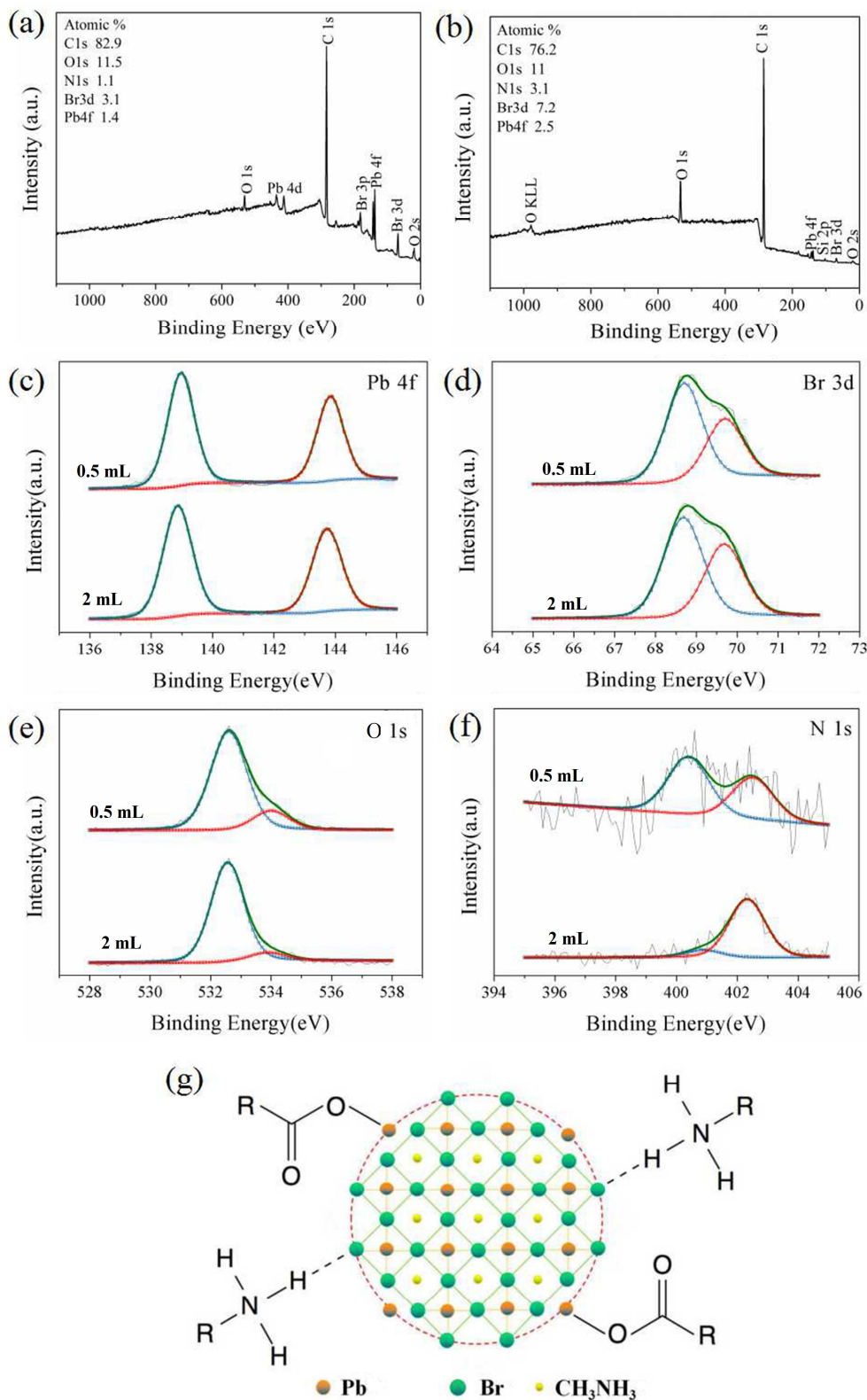


Fig. 4. XPS survey scans of PNCs synthesized with 0.5 mL (a) and 2 mL (b) precursor solution. (c-f) High resolution XPS spectra of Pb 4f (c), Br 3d (d), O 1s (e) and N 1s (f) for the 0.5 mL and 2 mL samples. (g) Schematic representation of the ligand binding modes on the $\text{CH}_3\text{NH}_3\text{PbBr}_3$ PNC surface, including octylammonium cation binding to surface Br, and oleate anion binding to the surface Pb ions.

3.3. Stability of $\text{CH}_3\text{NH}_3\text{PbBr}_3$ PNCs

The stability of PNCs is vital for application in optoelectronic devices. To evaluate the stability of the synthesized $\text{CH}_3\text{NH}_3\text{PbBr}_3$ PNCs, the PNCs solutions were placed under the dark at room temperature, and the PL spectra were recorded after different storage periods in the open air as shown in Fig. 5. The absolute PLQYs were also measured and summarized in Table 1. For the 0.5 mL sample, the PL spectrum keeps almost constant during the test. After 30 days, no detectable decrease of PL intensity is observed. In addition, the initially observed 85% PLQY for the as-synthesized 0.5 mL sample shows only slight decrease with time and reaches a value of 78% after 15 days and 67% after 30 days, suggesting a high stability of the PNCs. The excellent stability is assigned to the low polarity of colloidal system which could protect the surface of PNCs and inhibit the agglomeration and degradation of particles. However, the 2 mL sample presents a fast decay of PL intensity with increase in time, e.g. the PL vanishes after 30 days. The concurrent decrease in PLQY is also observed. The initially observed 20% PLQY for 2 mL sample shows a considerable decrease with time and reaches a value of 5% after 15 days and totally quenches after 30 days, which is likely due to a complete degradation of the PNCs in the more polar mixture system.

Table 1. PLQYs obtained for the PNCs in different time intervals

Sample	PLQY(%) (As-synthesized)	PLQY(%) (15 days)	PLQY(%) (30 days)
0.5 mL	85	78	67
1 mL	58	53	12
2 mL	20	3	2

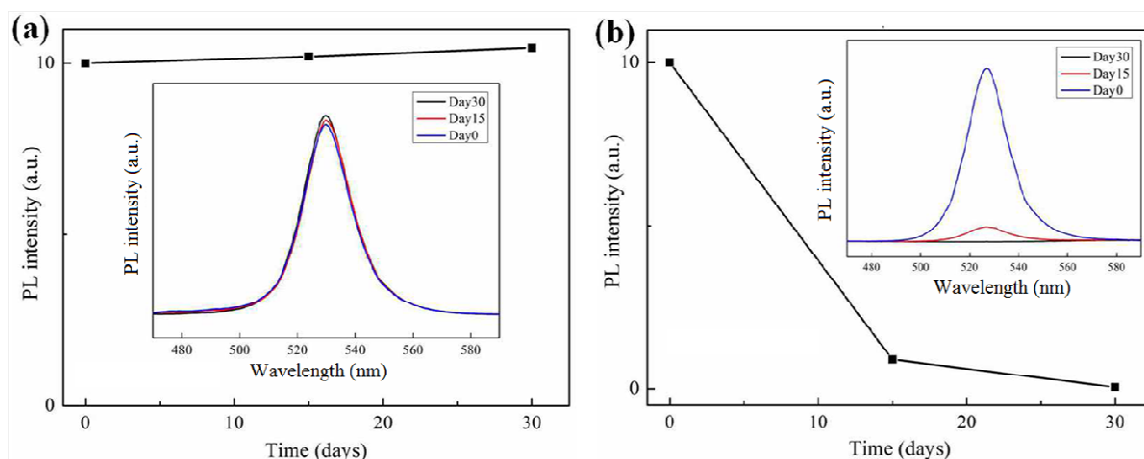


Fig. 5. PL intensity variation of $\text{CH}_3\text{NH}_3\text{PbBr}_3$ PNCs solution versus the storage time in the open air, and the inset shows the PL spectra of the PNCs measured after different days: (a) the 0.5 mL sample; (b) the 2 mL sample.

4. Conclusions

In summary, $\text{CH}_3\text{NH}_3\text{PbBr}_3$ PNCs were synthesized with variable PSV by LARP approach. All the PNCs exhibited spherical shape with narrow size distribution, green emission with narrow FWHM and small Stokes shift. 0.5 mL of PSV was found to yield highest PNCs concentration and excellent optical properties including high PLQY and good stability. Both the amount of precursor and the polarity of reaction system play important roles in the nucleation and growth of PNCs. At the lower PSV, few crystal nuclei are generated due to lower amount of precursor, which is favorable for the growth of large perovskite crystals. At the higher PSV, the inhibition of crystal growth with increased amount of precursor is compensated by increasing the polarity of mixture solvent, which leads to the dissolution of surface ligands and eventually growth of large perovskite crystals. In addition, PNCs obtained from high polar mixture exhibit substantially lowered PLQY and stability in air. The obtained results on dual-factor effect on nucleation and growth of PNCs will be very instructive for further studies in the LARP process.

Acknowledgements

The work was supported by the National Natural Science Foundation of China (NSFC Grants 51704225).

References

- [1] B. Lee, J. He, R.P. Chang, M.G. Kanatzidis, All-solid-state dye-sensitized solar cells with high efficiency, *Nature*, 485 (2012) 486-489.
- [2] J.H. Im, J.S. Luo, M. Franckevičius, N. Pellet, P. Gao, T. Moehl, S.M. Zakeeruddin, M.K. Nazeeruddin, M. Grätzel, N.G. Park, Nanowire perovskite solar cell, *Nano Lett.*, 15 (2015) 2120-2126.
- [3] S.S. Mali, C.S. Shim, C.K. Hong, Highly stable and efficient solid-state solar cells based on methylammonium lead bromide ($\text{CH}_3\text{NH}_3\text{PbBr}_3$) perovskite quantum dots, *NPG Asia Mater.*, 7 (2015) e208.
- [4] A. Kojima, K. Teshima, Y. Shirai, T. Miyasaka, Organometal halide perovskites as visible-light sensitizers for photovoltaic cells, *J. Am. Chem. Soc.*, 131 (2009) 6050-6051.
- [5] X.F. Zeng, T.W. Zhou, C.Q. Leng, Z.G. Zang, M. Wang, W. Hu, X.S. Tang, S. Lu, L. Fang, M. Zhou, Performance improvement of perovskite solar cell by employing CdSe quantum dot/PCBM composite as electron transport layer, *J. Mater. Chem. A*, 5 (2017) 17499-17505.
- [6] M. Wang, Z.G. Zang, B. Yang, X.F. Hua, K. Sun, L.D. Sun, Performance improvement of perovskite solar cells through enhanced hole extraction: The role of iodide concentration gradient, *Sol. Energ. Mat. Sol. C.*, 185 (2018) 117-123.
- [7] J. Xing, F. Yan, Y.W. Zhao, S. Chen, H.K. Yu, Q. Zhang, R.G. Zeng, H.V. Demir, X.W. Sun, A. Huan, Q.H. Xiong, High-efficiency light-emitting diodes of organometal halide perovskite amorphous nanoparticles, *ACS Nano*, 10 (2016) 6623-6630.
- [8] Z.K. Tan, R.S. Moghaddam, M.L. Lai, P. Docampo, R. Higler, F. Deschler, M. Price, A. Sadhanala, L.M. Pazos, D. Credgington, F. Hanusch, T. Bein, H.J. Snaith,

- R.H. Friend, Bright light-emitting diodes based on organometal halide perovskite, *Nat. Nanotechnol.*, 9 (2014) 687-692.
- [9] F. Zhang, H.Z. Zhong, C. Chen, X.G. Wu, X.M. Hu, H.L. Huang, J.B. Han, B.S. Zou, Y.P. Dong, Brightly luminescent and color-tunable colloidal $\text{CH}_3\text{NH}_3\text{PbX}_3$ (X= Br, I, Cl) quantum dots: potential alternatives for display technology, *ACS Nano*, 9 (2015) 4533-4542.
- [10] S.A. Veldhuis, P.P. Boix, N. Yantara, M.J. Li, T.C. Sum, N. Mathews, S.G. Mhaisalkar, Perovskite materials for light-emitting diodes and lasers, *Adv. Mater.*, 28 (2016) 6804-6834.
- [11] B.R. Sutherland, E.H. Sargent, Perovskite photonic sources, *Nat. Photonics*, 10 (2016) 295-302.
- [12] W. Xu, F.M. Li, Z.X. Cai, Y.R. Wang, F. Luo, X. Chen, An ultrasensitive and reversible fluorescence sensor of humidity using perovskite $\text{CH}_3\text{NH}_3\text{PbBr}_3$, *J. Mater. Chem. C*, 4 (2016) 9651-9655.
- [13] C. Liu, K. Wang, C. Yi, X.J. Shi, P.C. Du, A.W. Smith, A. Karim, X. Gong, Ultrasensitive solution-processed perovskite hybrid photodetectors, *J. Mater. Chem. C*, 3 (2015) 6600-6606.
- [14] S.F. Zhuo, J.F. Zhang, Y.M. Shi, Y. Huang, B. Zhang, Self-template-directed synthesis of porous perovskite nanowires at room temperature for high-performance visible-light photodetectors, *Angew. Chem., Int. Ed.*, 54 (2015) 5693-5696.
- [15] J.A. Sichert, Y. Tong, N. Mutz, M. Vollmer, S. Fischer, K.Z. Milowska, R.G. Cortadella, B. Nickel, C. Cardenas-Daw, J.K. Stolarczyk, A.S. Urban, J. Feldmann, Quantum size effect in organometal halide perovskite nanoplatelets, *Nano Lett.*, 15 (2015), 6521-6527.
- [16] L.C. Schmidt, A. Pertegás, S. González-Carrero, O. Malinkiewicz, S. Agouram, G.M. Espallargas, H.J. Bolink, R.E. Galian, J. Pérez-Prieto, Nontemplate synthesis of $\text{CH}_3\text{NH}_3\text{PbBr}_3$ perovskite nanoparticles, *J. Am. Chem. Soc.*, 136 (2014) 850-853.

- [17] O. Vybornyi, S. Yakunin, M.V. Kovalenko, Polar-solvent-free colloidal synthesis of highly luminescent alkylammonium lead halide perovskite nanocrystals, *Nanoscale*, 8 (2016) 6278-6283.
- [18] H. Huang, A.S. Susa, S.V. Kershaw, T.F. Hung, A.L. Rogach, Control of emission color of high quantum yield $\text{CH}_3\text{NH}_3\text{PbBr}_3$ perovskite quantum dots by precipitation temperature, *Adv. Sci.*, 2 (2015) 1500194.
- [19] H. Huang, J. Raith, S.V. Kershaw, S. Kalytchuk, O. Tomanec, L.H. Jing, A.S. Susa, R. Zboril, A.L. Rogach, Growth mechanism of strongly emitting $\text{CH}_3\text{NH}_3\text{PbBr}_3$ perovskite nanocrystals with a tunable bandgap, *Nat. Commun.*, 8 (2017) 996.
- [20] L. Peng, A.W. Tang, C.H. Yang, F. Teng, Size-controlled synthesis of highly luminescent organometal halide perovskite quantum dots, *J. Alloy. Compd.*, 687 (2016) 506-513.
- [21] F. Zhu, L. Men, Y.J. Guo, Q.C. Zhu, U. Bhattacharjee, P.M. Goodwin, J.W. Petrich, E.A. Smith, J. Vela, Shape evolution and single particle luminescence of organometal halide perovskite nanocrystals, *ACS Nano*, 9 (2015) 2948-2959.
- [22] M.Y. Wei, W.H. Sun, Y. Liu, Z.W. Liu, L.X. Xiao, Z.Q. Bian, Z.J. Chen, Highly luminescent and stable layered perovskite as the emitter for light emitting diodes, *Phys. Status Solidi A*, 213 (2016) 2727-2732.
- [23] H.L. Huang, F.C. Zhao, L.G. Liu, F. Zhang, X.G. Wu, L.J. Shi, B.S. Zou, Q.B. Pei, H.Z. Zhong, Emulsion synthesis of size-tunable $\text{CH}_3\text{NH}_3\text{PbBr}_3$ quantum dots: An alternative route toward efficient light-emitting diodes, *ACS Appl. Mater. Inter.*, 7 (2015) 28128-28133.
- [24] T. Zhang, H.N. Chen, Y. Bai, S. Xiao, L. Zhu, C. Hu, Q.Z. Xue, S.H. Yang, Understanding the relationship between ion migration and the anomalous hysteresis in high-efficiency perovskite solar cells: A fresh perspective from halide substitution, *Nano Energy*, 26 (2016) 620-630.
- [25] S. Bhaumik, S.A. Veldhuis, Y.F. Ng, M.J. Li, S.K. Muduli, T.C. Sum, B. Damodaran, S. Mhaisalkar, N. Mathews, Highly stable, luminescent core-shell type methylammoniumoctylammonium lead bromide layered perovskite nanoparticles, *Chem. Commun.*, 44 (2016) 7118-7121.

- [26] V.A. Hintermayr, A.F. Richter, F. Ehrat, M. Döblinger, W. Vanderlinden, J.A. Sichert, Y. Tong, L. Polavarapu, J. Feldmann, A.S. Urban, Tuning the optical properties of perovskite nanoplatelets through composition and thickness by ligand-assisted exfoliation, *Adv. Mater.*, 28 (2016) 9478-9485.
- [27] V.K. Lamer, R.H. Dinegar, Theory, production and mechanism of formation of monodispersed hydrosols, *J. Am. Chem. Soc.*, 72 (1950) 4847-4854.
- [28] K. Tanaka, T. Takahashi, T. Ban, T. Kondo, K. Uchida, N. Miura, Comparative study on the excitons in lead-halide-based perovskite-type crystals $\text{CH}_3\text{NH}_3\text{PbBr}_3$ $\text{CH}_3\text{NH}_3\text{PbI}_3$, *Solid State Commun.*, 127 (2003) 619-623.
- [29] S. Gonzalez-Carrero, R.E. Galian, J. Pérez-Prieto, Maximizing the emissive properties of $\text{CH}_3\text{NH}_3\text{PbBr}_3$ perovskite nanoparticles, *J. Mater. Chem. A*, 3 (2015) 9187-9193.
- [30] J.A. Dean, in *Lange's Handbook of Chemistry 15th ed.*, McGraw-Hill Inc., New York, USA, 1999.
- [31] S. Chen, T.W. Goh, D. Sabba, J. Chua, N. Mathews, C.H.A. Huan, T.C. Sum, Energy level alignment at the methylammonium lead iodide/copper phthalocyanine interface, *APL Mater.*, 2 (2014) 081512.
- [32] S.A. Veldhuis, Y.K.E. Tay, A. Bruno, S.S.H. Dintakurti, S. Bhaumik, S.K. Muduli, M.J. Li, N. Mathew, T.C. Sum, S.G. Mhaisalkar, Benzyl alcohol-treated $\text{CH}_3\text{NH}_3\text{PbBr}_3$ nanocrystals exhibiting high luminescence, stability, and ultralow amplified spontaneous emission thresholds, *Nano Lett.*, 17 (2017) 7424-7432.
- [33] J. De Roo, M. Ibáñez, P. Geiregat, G. Nedelcu, W. Walravens, J. Maes, J.C. Martins, I.V. Driessche, M.V. Kovalenko, Z. Hens, Highly dynamic ligand binding and light absorption coefficient of cesium lead bromide perovskite nanocrystals, *ACS Nano*, 10 (2016) 2071-2081.
- [34] A.Z. Pan, B. He, X.Y. Fan, Z.K. Liu, J.J. Urban, A.P. Alivisatos, L. He, Y. Liu, Insight into the ligand-mediated synthesis of colloidal CsPbBr_3 perovskite nanocrystals: the role of organic acid, base, and cesium precursors, *ACS Nano*, 10 (2016) 7943-7954.

Highlights

- PSV was varied to modify precursor amount and polarity of mixture at the same time
- Concentration and optical properties of PNCs as a function of PSV were investigated
- The influence of the dual-factor on the nucleation and growth of PNCs was revealed